Computer Assisted Mechanics and Engineering Sciences, **13**: 547–556, 2006.

A new approach to physically based interpretation of experimental data in 2D problems in mechanics

Wojciech Karmowski, Grzegorz Midura
Cracow University of Technology, ul. Warszawska 24, 31-155 Kraków, Poland

(Received in the final form October 6, 2006)

The concept of experimental data interpretation in mechanics using Dirac function is presented. The objective is to find general differential equation, which may be used to approximate the stress field sought. Application of this method may convert problem from general spline to variational one. Basic idea has been presented earlier in [6] where both theoretical data and results of experiments have been taken into account. Here, the method has been used to solve a 2D problem. Numerical tests performed for both generated and experimental data proved its usefulness.

1. Introduction

Experimental measurements in mechanics are usually carried out on the surface of the analysed body. Due to very high cost and extremely complicated equipment needed for 3D experiments such analysis is performed rather seldom [10]. Therefore the method presented here has been prepared to solve 2D problems although proposed algorithm could be generalised onto 3D space using Maxwell functions instead of Airy function.

The general problem of restoring stress tensor by using experimental data has been discussed many times before e.g. [4, 6, 8, 9].

Data measured in experiment is always obtained at separate points. Usually because of significant costs, physical constraints and other reasons, number of measurement points is minimized. Moreover, measurements are disturbed by experimental errors and usually this error is difficult to estimate.

Therefore presented algorithm has to fulfill two goals of post-experimental analysis:

- extend data to the whole analysed area,
- improve data in order to minimize experimental errors.

Stress field almost always satisfies equilibrium equations, which should be taken into account [6]. Usually one additionally has to deal with boundary conditions. All this information may be treated together by proper definition of the functional, containing all available data. Minimization of this functional leads to the optimal stress field distribution. This may be achieved by a transformation of the relevant functional having general spline character [1] to a variational one [4]. Euler equation thus becomes a differential equation for a certain new problem. Solutions may be recognized as a representation of the relevant stress problem.

Due to small equation system (depending only on number of measurements), presented algorithm is very fast and efficient and therefore requires a small amount of computational time. For this reason the presented method does not require special computer hardware and can be widely used in processing of experimental results. The proposed method is physically based (satisfies equilibrium equation) and the obtained solution covers the whole analysed area.

2. Mathematical formulation

In this case general spline functional takes into account both certain theoretical relationships and experimental data, and may be expressed as a following functional of unknown function "f"

$$\Phi(f,\lambda) := \Lambda + \lambda \sum_{n=1}^{N} \alpha_n \Theta_n(f) \tag{1}$$

where N is the number of experiments, parameters α_n are introduced to weight the relative share of measurements Θ, which may have different physical types. Parameter λ is introduced to weight the theoretical (Λ) and experimental (Θ) parts. Minimization of such a functional leads to smooth and physically based stress field.

The theoretical part of Eq. (1) in solid mechanics may be obtained from equilibrium equation, i.e. if f is the searched stress tensor, then if Ω denotes the analysed domain:

$$\Lambda(\breve{\sigma}) = \int_{\Omega} (\operatorname{div} \breve{\sigma})^2 \, \mathrm{d}\Omega \tag{2}$$

Equation (2) represents mean quadratic error of equilibrium equations. Alternatively, f may be defined as an Airy function. This ensures fulfillment of basic rules of mechanics such as equilibrium equations,

$$\frac{\partial \sigma_{xx}}{\partial x} + \frac{\partial \sigma_{xy}}{\partial y} = 0\,, \qquad \frac{\partial \sigma_{xy}}{\partial x} + \frac{\partial \sigma_{yy}}{\partial y} = 0\,. \tag{3}$$

When f is defined as the Airy function, Λ may be an universal measure of field curvature. In [4] this curvature was proposed as

$$\Lambda(f) = \int_{\Omega} \kappa^2(f) \, \mathrm{d}\Omega \tag{4}$$

and κ as

$$\kappa = \sqrt{\frac{1}{2\pi} \int_0^{2\pi} \left(\frac{\partial^2 f}{\partial \vec{r}^2} \right)^2 \mathrm{d}\varphi}\,. \tag{5}$$

Experimental parts of the functional can take the form

$$\Theta_n(\breve{\sigma}) = D_n \left\| \breve{\sigma}(\vec{r}_n) - \breve{s}_n \right\|^2 , \tag{6}$$

where

$$\|\breve{\sigma}\| = (\operatorname{tr} \breve{\sigma}^2)^{1/2} \tag{7}$$

to represent the discrepancy between measured and approximated data, where D_n is a local weighting factor, $\breve{s}_n$ is the measured stress tensor (e.g. by strain gauges).

The experimental term of the functional may be converted to the surface integral all over the domain if each sought value at a given point will be multiplied by the Dirac pseudo-function

$$\delta(\vec{r}) = 0 \qquad \text{for} \quad \vec{r} \neq 0 \tag{8}$$

and with the condition

$$\int_V \delta(\vec{r}) \, \mathrm{d}V = 1 \tag{9}$$

centered at the analysed point, where V represents the whole space. Minimization of the functional (1) leads to the following equation (in the case of Airy function version):

$$\Delta^4 f + \lambda \sum_n \alpha_n D_n \left(\breve{\sigma}(\vec{r}_n) - \breve{s}_n \right)_{ij} \partial_{ij} \, \delta(\vec{r} - \vec{r}_n) = 0. \tag{10}$$

The Airy function may be now presented as

$$f(\vec{r}) = \lambda \sum_n D_n \gamma_{,ij}(\vec{r} - \vec{r}_n)\, w_{nij} + f^*(\vec{r}) \tag{11}$$

where:

$$\gamma(\vec{r}) = \begin{cases} 0 & r = 0, \\ \frac{r^6}{4608\pi}\left(\ln r - \frac{5}{6}\right) & r > 0, \end{cases} \tag{12}$$

and

$$w_{nij} = -(\partial_{ij} f)(\vec{r}_n) + s_{nij}\,. \tag{13}$$

The first term of Eq. (11) constitutes a sum of arbitrary solution of above equation and a general, homogeneous square-biharmonical function (f^*), which may be presented as a linear combination of basic solutions $\tilde{G}$, s_{ij} are components of known, measured stresses. The proposed stress field obtained from the Airy function (11) at point $\vec{r}_n$ is the same as $\breve{\sigma}(\vec{r}_n)$. This leads to a system of $3N$ linear equations

$$w_{nij} + \lambda \sum_{\acute{n}} D_{\acute{n}} G_{ij,\acute{i}\acute{j}}(\vec{r}_n - \vec{r}_{\acute{n}}) a_{\acute{i}\acute{j}} = s_{nij} \tag{14}$$

where the tensor $G(r, \varphi)$ satisfies the following relationships:

$$\begin{aligned}
G_{xx,xx} &= \frac{r^2}{768\pi}\left(\ln r(48\cos^2\varphi + 12) + 8\cos^4\varphi - 4\sin^2\varphi - 1\right), \\
G_{xx,xy} &= G_{xy,xx} = \frac{r^2}{384\pi}\sin\varphi\cos\varphi(12\ln r + 4\cos^2\varphi + 1), \\
G_{xy,xy} &= G_{xx,yy} = G_{yy,xx} = \frac{r^2}{768\pi}\left(12\ln r\cos^2\varphi(8\sin^2\varphi - 1) - \sin^2\varphi\right), \\
G_{xy,yy} &= G_{yy,xy} = \frac{r^2}{384\pi}\sin\varphi\cos\varphi(12\ln r + 4\sin^2\varphi + 1), \\
G_{yy,yy} &= \frac{r^2}{768\pi}\left(\ln r(48\sin^2\varphi + 12) + 8\sin^4\varphi - 4\cos^2\varphi - 1\right).
\end{aligned} \tag{15}$$

Such a value of λ is proposed to ensure minimization of a'posteriori error norm determined as a difference between computed and measured values, i.e. of the second part of Eq. (1).

3. Benchmark tests

3.1. Test for generated data (known solution)

Approximations obtained for different values of parameter λ are compared with the known, exact solution. Pseudo-experimental points shown in Fig. 1 are generated randomly in 2D.

Values of stresses at these points have been generated using testing Airy function

$$F(x, y) = -2A\frac{\cos^2\left(\pi p\frac{x}{2}\right)\cos^2\left(\pi p\frac{y}{2}\right)}{\pi^2 p^2}\,, \tag{16}$$

for A and p assumed arbitrarily. For such a function F, stress tensor components s_{xx}, s_{xy} and s_{yy} may be found easily:

$$\begin{aligned}
s_{xx}(x, y) &= A\cos(\pi py)\left(\frac{\cos(\pi px)}{2} + \frac{1}{2}\right), \\
s_{xy}(x, y) &= \frac{A}{2}\sin(\pi px)\sin(\pi py), \\
s_{yy}(x, y) &= A\cos(\pi px)\left(\frac{\cos(\pi py)}{2} + \frac{1}{2}\right).
\end{aligned} \tag{17}$$

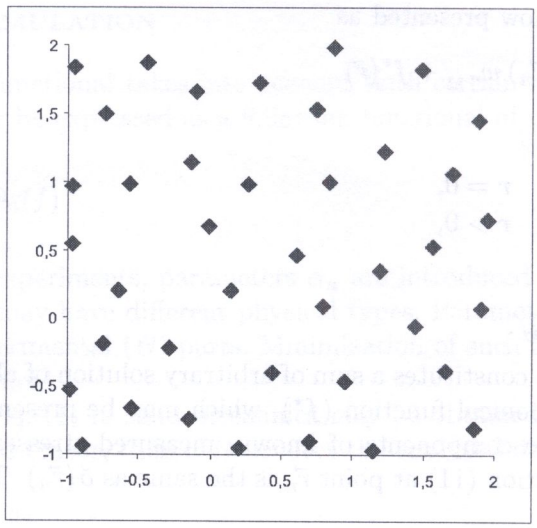

Fig. 1. Pseudo–experimental points

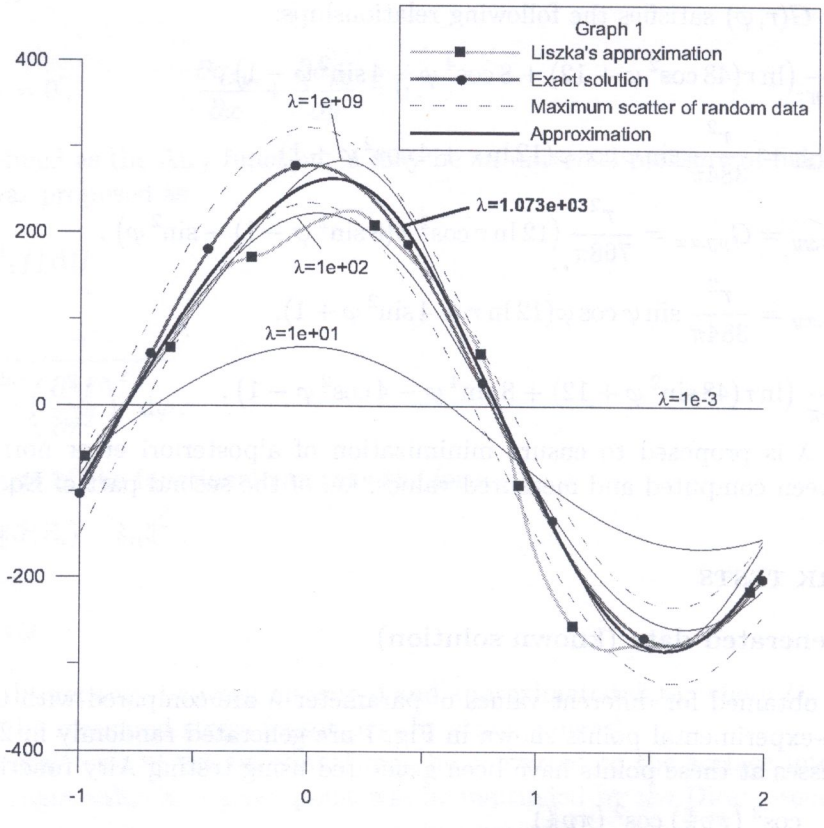

Fig. 2. Difference between exact solution and approximation in L2 norm due to various parameters λ

Parameters $p = \frac{1}{2}$, $A = 1000$ have been assumed for further calculations. After generation, data has been disturbed randomly at each point of measurement n, separately for each stress component s_{ij} using random value the range of (-20%,20%).

This test has been conducted for various values of parameter λ and obtained approximation has been compared with exact solution in L2 norm. Approximations for s_{xx} stress component, $y = 0.5$ and different values of parameter λ have been shown in Fig. 2. These results were compared with the exact value and Liszka's approximation [7].

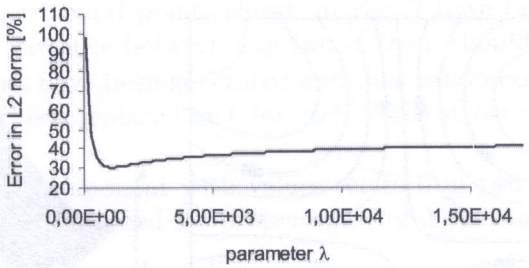

Fig. 3. Approximation for different values of parameter λ

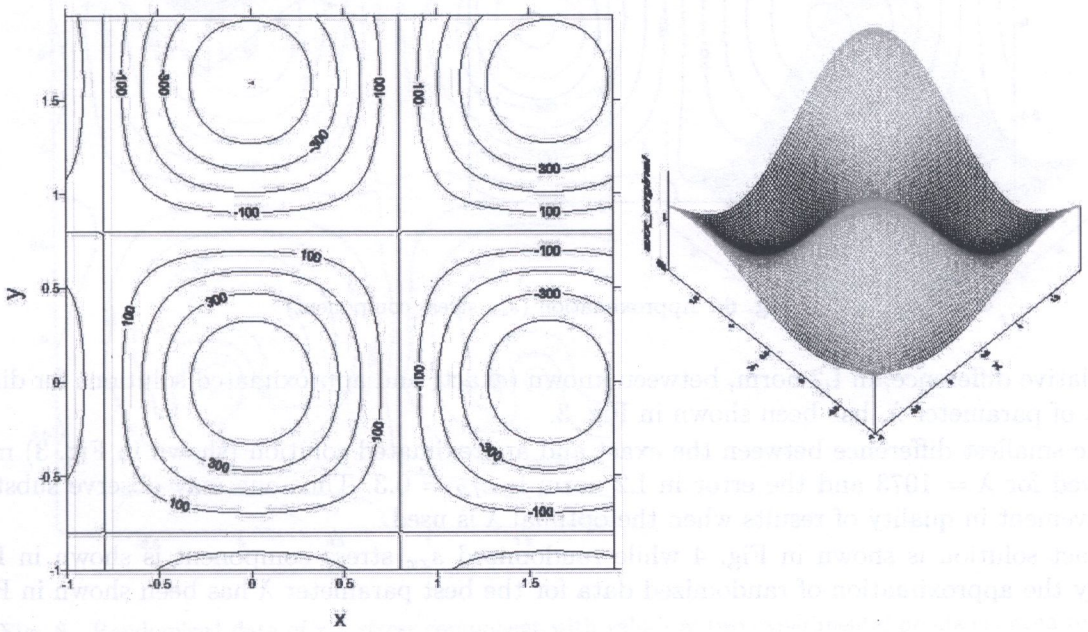

Fig. 4. Exact solution (s_{xx} stress component)

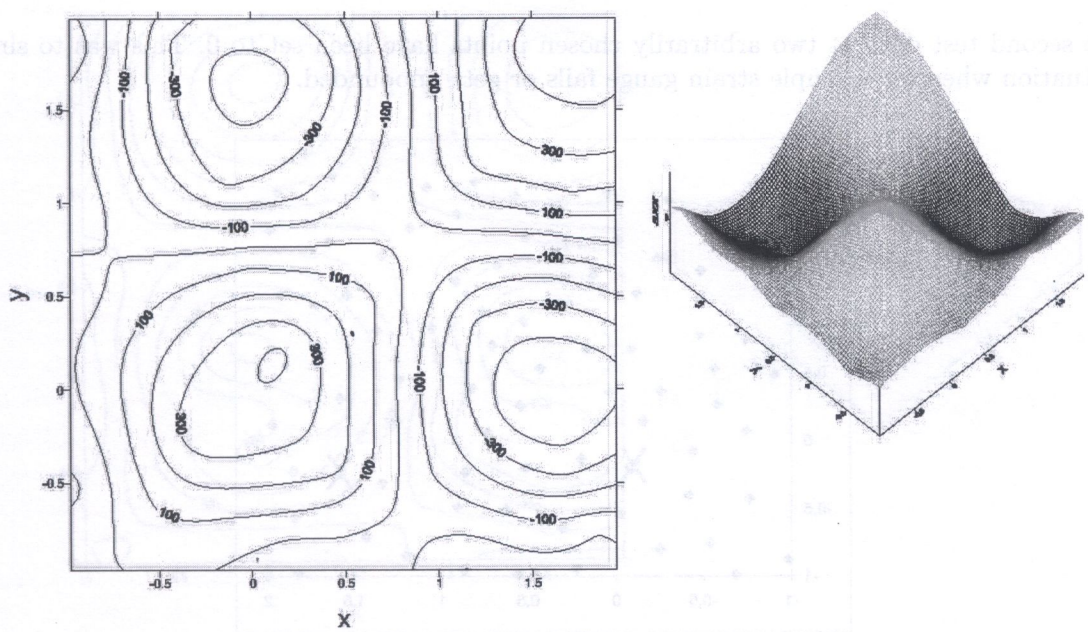

Fig. 5. Randomized data (s_{xx} stress component)

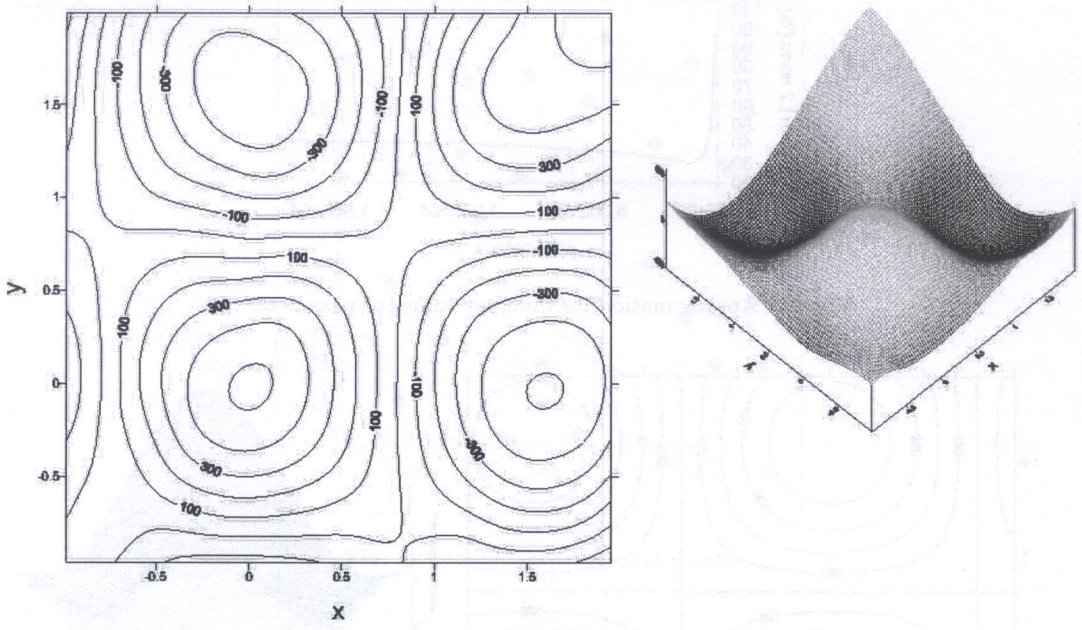

Fig. 6. Approximation (s_{xx} stress component)

Relative difference, in L2 norm, between known (exact) and approximated solutions for different values of parameter λ, has been shown in Fig. 3.

The smallest difference between the exact and approximated solution (shown in Fig. 3) may be observed for $\lambda = 1073$ and the error in L2 norm is $e_{L2} = 0.3$. Thus one may observe substantial improvement in quality of results when the optimal λ is used.

Exact solution is shown in Fig. 4 while randomized s_{xx} stress component is shown in Fig. 5. Finally the approximation of randomized data for the best parameter λ has been shown in Fig. 6.

3.2. Test for generated data (original values set to 0 in 2 points)

In the second test data at two arbitrarily chosen points have been set to 0. This was to simulate the situation when for example strain gauge fails or gets unbounded.

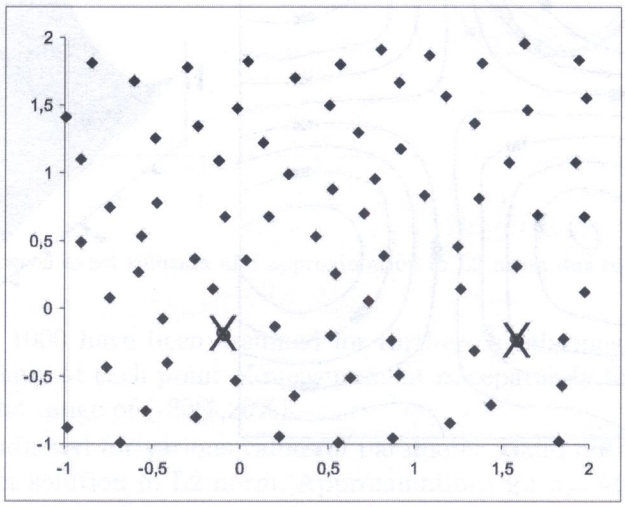

Fig. 7. Experimental points

For this test $N = 80$ experimental points shown in Fig. 7 have been generated randomly, but satisfying the condition that distance between any two of them should not be too small.

Values of stress components have been generated and then randomized at points shown in Fig. 7. Finally obtained values have been replaced by 0 for each of the stress components at points marked with X.

The randomized s_{xx} stress component with values set to 0 in two arbitrary points is shown in Fig. 8, the best approximation (obtained for proper value of λ) is shown in Fig. 9 while the exact solution is presented in Fig. 10.

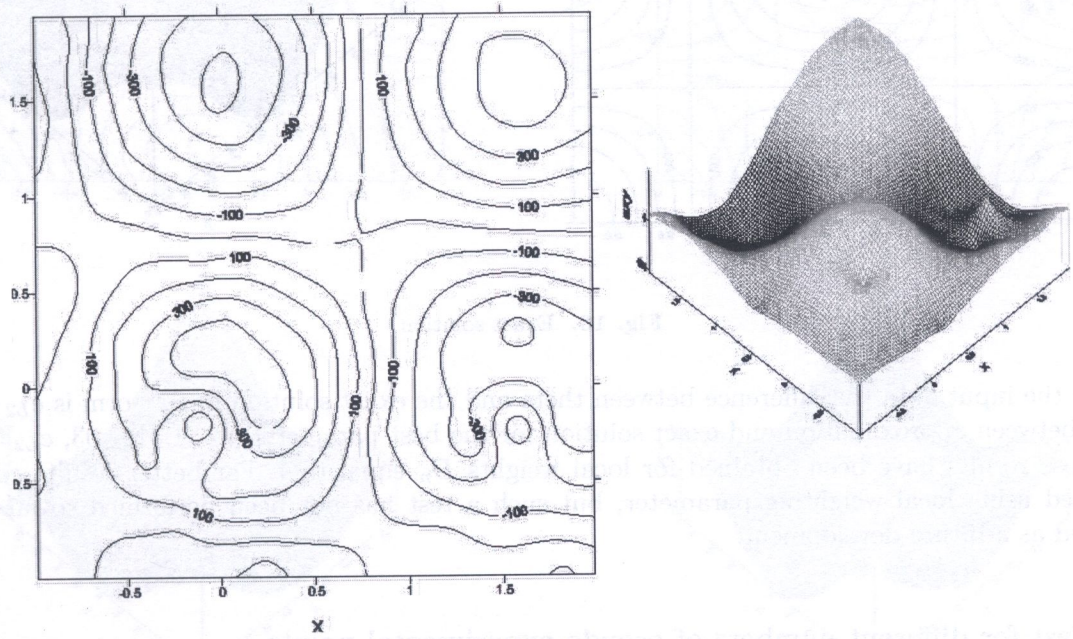

Fig. 8. Randomized data of s_{xx} stress component with values in two experimental points changed to 0

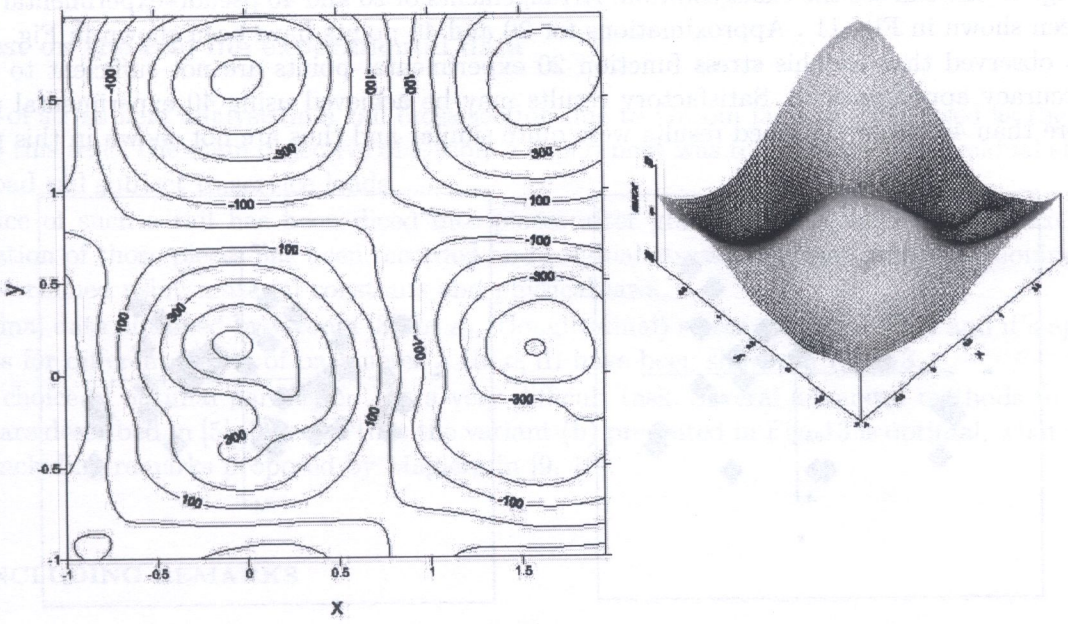

Fig. 9. Data approximation (s_{xx} stress component)

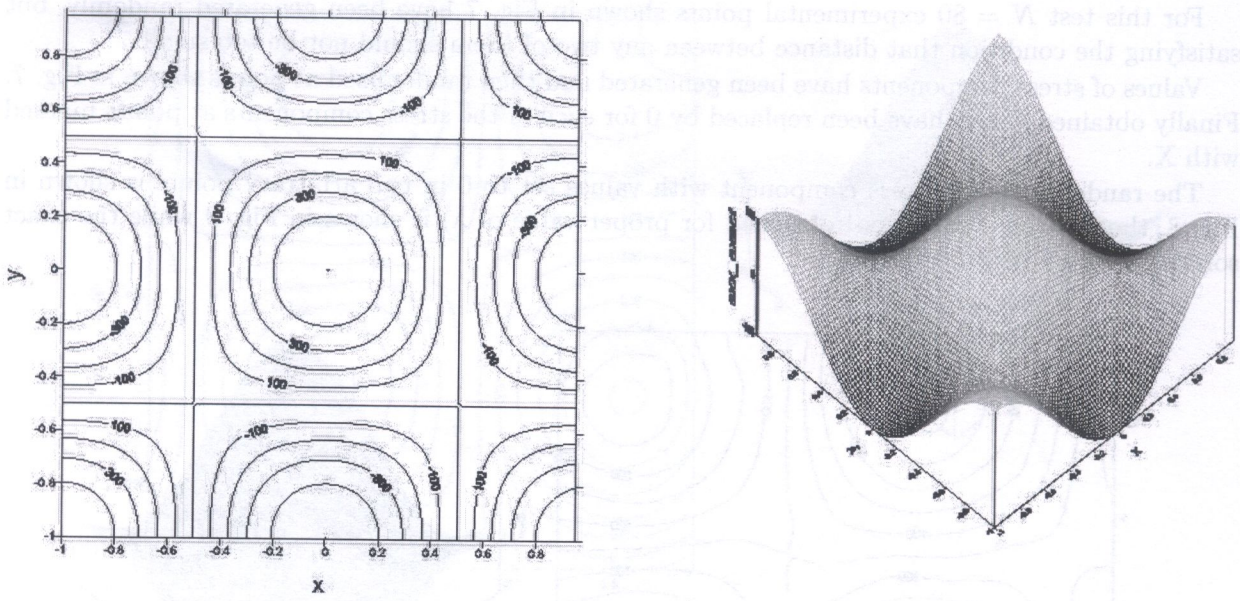

Fig. 10. Exact solution

For the input data the difference between them and the exact solution in L2 norm is $e_{L2} = 0.62$ while between approximation and exact solution for the best parameter $\lambda = 1.01\text{e}{+03}$, $e_{L2} = 0.46$.

Those results have been obtained for local weights D_n equal to 1. Far better results could be obtained using local weighting parameter, but such a test has not been performed so far and is planned as a future development.

3.3. Test for different numbers of pseudo-experimental points

In this test approximation has been obtained for different numbers of pseudo-experimental points. Test was begun with 20 and ended with 160 experimental points.

In Fig. 10 one can see the exact solution. Arrangements of 20 and 40 pseudo-experimental points have been shown in Fig. 11 . Approximations for 20 and 40 points have been shown in Fig. 12.

It is observed that for this stress function 20 experimental points are not sufficient to obtain high accuracy approximation. Satisfactory results may be achieved using 40 experimental points. For more than 40 points obtained results were quite similar and thus are not shown in this paper.

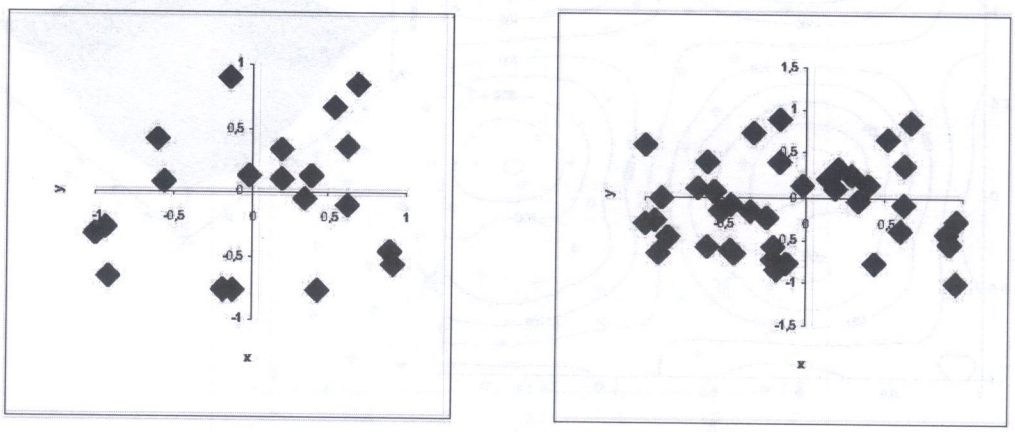

Fig. 11. Arrangement of 20 and 40 pseudo-experimental points

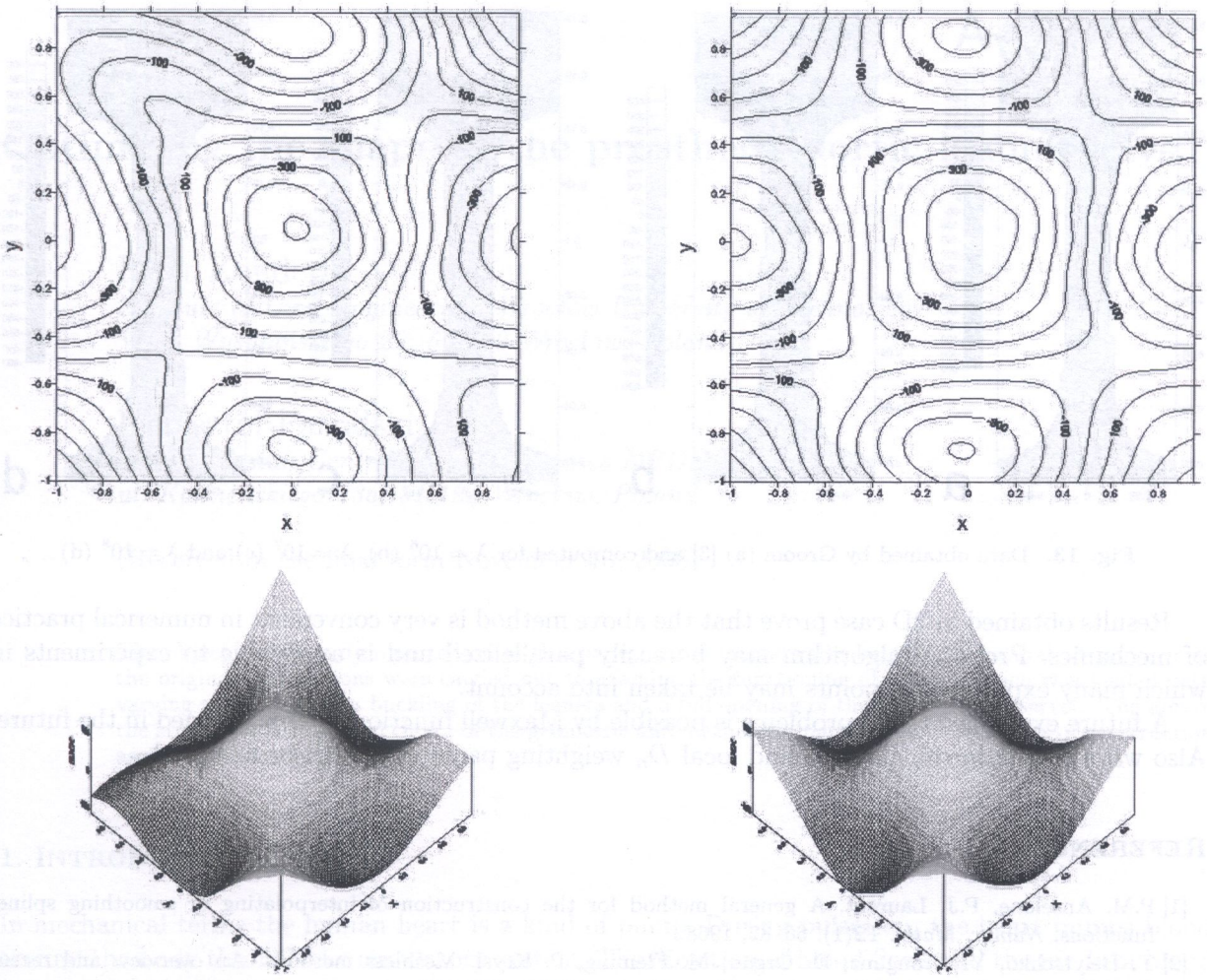

Fig. 12. Approximation for 20 and 40 pseudo-experimental points (s_{xx} stress component)

3.4. Test on the real life experimental data

Results of stress field analysis in a rail cross-section due to Groom [3] have been used as the input data for this test. The main objective of Groom's experiment was to determine the residual stresses in railroad rail subject to service loads.

A slice of such a rail has been diced into pieces after gluing strain gauges to it's face. Thus deformation of those pieces has been recorded and residual stresses released during sectioning have been determined using material constants and physical laws.

Original data obtained by Groom [3] for s_{xx} (longitudinal) stress component (a) and it's approximations for different values of parameter λ (b, c, d) have been shown in Fig. 13.

The choice of optimal parameter λ is a very difficult task. Several advanced methods to determine λ are described in [5]. It seems that the variant (b) presented in Fig. 13 is optimal, what agrees with concluding remarks proposed by Magiera in [9, 10].

4. Concluding remarks

The paper presents a new idea of experimental data approximation that takes into consideration general equations of mechanics, algorithm is very fast and efficient.

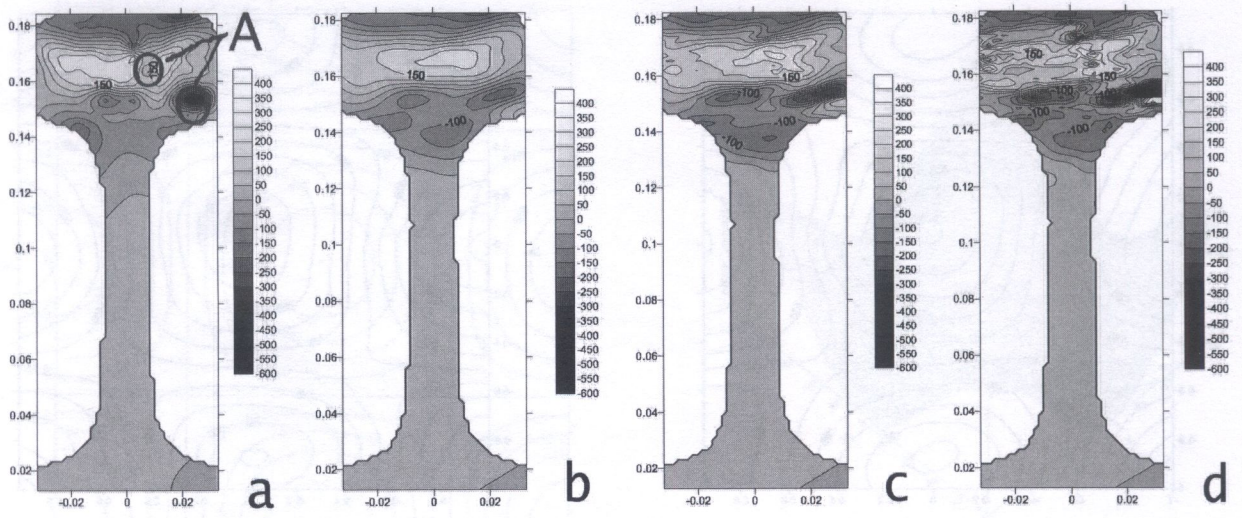

Fig. 13. Data obtained by Groom (a) [3] and computed for $\lambda = 10^6$ (b), $\lambda = 10^7$ (c) and $\lambda = 10^8$ (d)

Results obtained in 2D case prove that the above method is very convenient in numerical practice of mechanics. Proposed algorithm may be easily parallelized and is applicable to experiments in which many experimental points may be taken into account.

A future expansion to 3D problems is possible by Maxwell functions and is planned in the future. Also ways to obtain the global λ and local D_n weighting parameters will be analysed.

References

[1] P.M. Anselone, P.J. Laurent. A general method for the construction of interpolating or smoothing spline-functions. *Numer. Math.*, **12**(1): 66–82, 1968.

[2] T. Belytschko, Y. Krongauz, D. Organ, M. Fleming, P. Krysl. Meshless methods: An overview and recent developments. *Comput. Methods Appl. Mech. Engrg.*, **139**: 3–47, 1996.

[3] J.J. Groom. *Determination of residual stresses in rails.* Final report to the US DOT No.DOT/FRA/ORD–83/05, Columbus, OH, 1983.

[4] W. Karmowski. Application of the Dirac function to experimental data interpretation in solid mechanics. *XIV Polish Conference on Computer Methods in Mechanics,* Rzeszów, 145–146, 1999.

[5] W. Karmowski. *Wspomagana teorią interpretacja wyników eksperymentów mechaniki ciał odkształcalnych.* Monografia PK, **251**, Kraków 1999.

[6] W. Karmowski, J. Orkisz. A physically based method of enhancement of experimental data – concepts, formulation and application to identification of residual stresses. *Inverse Problems in Engineering Mechanics*, pp 61–70. Springer-Verlag, 1993.

[7] T. Liszka. An interpolation method for an irregular net of nodes. *Int. J. Num. Meth. Engrg.*, **20**: 1599–1612, 1984.

[8] S.A. Łukasiewicz, M. Stanuszek, J.A. Czyż. Filtering of the experimental data in plane stress and strain fields. *Experimental Mechanics,* 139–147, June 1993.

[9] J. Magiera, J. Orkisz, W. Karmowski. Reconstruction of residual stresses in railroad from measurements made on vertical and oblique slices. *WEAR*, **191**: 78–89, 1996.

[10] J. Magiera, Enhanced 3D analysis of residual stress in rails by physically based fit to neutron diffraction data. *WEAR*, **253**: 228–240, 2002.